Earth and Planetary Science Letters, 26 (1975) 277–286

PYROXENES IN THE SYSTEM $Mg_2Si_2O_6$–$CaMgSi_2O_6$ AT HIGH PRESSURE

TAKESHI MORI and DAVID H. GREEN

Research School of Earth Sciences, Australian National University, Canberra, A.C.T. (Australia)

Received November 22, 1974
Revised version received May 2, 1975

The enstatite–diopside solvus in the system $Mg_2Si_2O_6$–$CaMgSi_2O_6$ has been experimentally determined within the pressure range 5–40 kbars and the temperature range 900–1500°C. Experiments involving reversal of the phase boundaries by unmixing from glass starting material and by reaction of pure clinoenstatite and diopside showed difficulty in achieving equilibration due to persistence of metastable, subcalcic clinopyroxene and to the sluggishness of reaction rate. The experimental data showed that the temperature dependence of the diopside limb is less than previously accepted. At 1500°C and 30 kbars subcalcic diopside found by Davis and Boyd (1966) is shown to be metastable with respect to enstatite and more calcic diopside of composition $En_{42.3}Di_{57.7}$. The solvus widens with increasing pressure between 5 and 40 kbars at 1200°C, but at 900°C the pressure effect on the solvus is very small. The stability relationships of the four pyroxenes, protoenstatite, enstatite, iron-free pigeonite and diopside are summarized, based on data from the literature and the present study.

1. Introduction

Previous studies [1–7] have shown that the solvus between enstatite and diopside in the system $Mg_2Si_2O_6$–$CaMgSi_2O_6$ narrows with increasing temperature and suggest that the pressure effect on the solvus is small and may be opposite to that of temperature. However, because of the possible uncertainty of measurement and some scattering of the experimental data, the pressure effect on the solvus remains uncertain. A further problem at high pressure and temperature is the strong curvature of the diopside limb above 1400°C at 30 kbars [4] with diopside becoming subcalcic ($En_{70}Di_{30}$ in mole %, at 1500°C and 30 kbars). Kushiro [3] suggested that these subcalcic clinopyroxenes might be pigeonitic.

In the present investigation we have concentrated our experiments on accurate determination of the pressure effect on the solvus from 5 to 40 kbars at 1200°C and on delineation of the temperature dependence of the solvus at 30 kbars. The practicability of the project was also dependent on the high accuracy and reproducibility of analysis on small grains, combined with excellent optics and contemporaneous analysis for all elements attainable with TPD electron probe and energy dispersive analytical system [8].

2. Preparation of starting materials

Several kinds of starting materials were prepared.

2.1. $En_{50}Di_{50}$ glass

Three separate glasses of the same composition, $En_{50}Di_{50}$ (mole %), were prepared from A.R. grade chemicals of SiO_2, MgO, and $CaCO_3$. Weighed mixtures of the reagents were melted on an iridium-strip heater and were stirred by a platinum rod to homogenize, then quenched by cutting off the power and simultaneously cooling by compressed air. The glasses were ground to average 25-μm grain size. One piece of glass from each batch was polished and examined by microscope, microprobe and, in some cases, X-ray powder photography. Two batches among the three

contained a trace amount (<1%) of quench clinopyroxene and olivine. Compositions of quenched clinopyroxene were similar to those of the host glasses. The third glass was free from any crystals. Composition of the three glasses varied from $En_{48.4}Di_{51.6}$ to $En_{49.6}Di_{50.4}$ with an inhomogeneity of ±0.2 to ±0.5 mole % end member.

2.2. $En_{80}Di_{20}$ glass

A glass with the composition of $En_{80}Di_{20}$ was made in the same way as above. A trace amount of crystals (≪1%) was found in the glass, but they were not identified because of their scarcity and tiny sizes. Analyzed composition of the glass was $En_{81.6}Di_{18.4}$.

2.3. Synthetic pyroxenes

In some homogenization runs, synthetic diopside ($CaMgSi_2O_6$) and clinoenstatite ($Mg_2Si_2O_6$) of Tem-Pres Research Co. were used. Microprobe analysis showed the presence of trace amount of CaO (<0.05 wt.%) in the clinoenstatite.

3. Synthesis and chemical analysis of pyroxenes

The high-pressure apparatus used was a Boyd and England [9] design piston-cylinder device and a pressure correction of −10% of nominal load pressure, using piston-in technique, was applied. This method of correction is based on calibrations on quartz-coesite at 1100°C [10] and albite = jadeite + quartz at 600°C (G. Brey and D.H. Green, unpublished data). Temperature measurement was by $Pt/Pt_{90}Rh_{10}$ thermocouple with no correction applied for pressure effect on thermocouple emf. Samples were encased in sealed Pt capsules or in Pt capsules with a crimped end in those cases where the catalytic effect of low water-vapour pressures was desired.

Chemical analyses were by means of the TPD-electron probe, with an analysis area of about 3 μm diameter as judged by fluorescence on periclase. The visible fluorescence of the pyroxenes made positioning for analysis easier and more reliable. All relevant elements were measured simultaneously and at least ten analyses were made on each pyroxene phase in every run. Some analyses with structural formulae deviating from stoichiometry were discarded. These were less than 10% of all the analyses.

In some of the homogenization experiments the capsule was loaded with a layer of clinoenstatite in contact with a layer of diopside. A polished thin section across this contact was prepared after the run and the contact between the two pyroxene types was examined optically and with the electron probe.

4. Experimental results

The run procedures, products and pyroxene compositions are summarized (Table 1 and brief comments in the Appendix). Pyroxene analyses* are shown (Fig. 1) except for the runs 2, 3 and 7 which are of shorter reaction time.

The spread of data in some of the unmixing and homogenization experiments is related to mechanisms and sluggishness of chemical reactions. As shown in run 2, the $En_{50}Di_{50}$ glass crystallized both orthopyroxene and clinopyroxene within only 6 minutes at 30 kbars and 1200°C. The glasses found in other experiments with longer run duration are, therefore, not unreacted starting glasses but melts generated by presence of water and equilibrated with pyroxenes. The water-saturated melting point of $En_{50}Di_{50}$ is about 1050°C at 30 kbars [7], and water added to or allowed to enter the capsules naturally causes melting at higher temperature. The run duration of 45 minutes at 30 kbars and 1200°C (run 3, Table 1) crystallized orthopyroxene and clinopyroxene of compositions lying between the original bulk composition and the equilibrium compositions. The 4-hour experiment (run 4) gave pyroxenes with a wider composition gap and appears to have reached the equilibrium compositions (see later discussion). Comparison of runs 7 and 8 shows a similar time dependent relationship for pyroxenes crystallizing from glass starting material. Although from these experiments we have no information on the initial steps of crystallization from glass, since even after 6 minutes we have two pyroxenes present, we have obtained further information in Fe-bearing experiments with varying run duration. The crystallization sequence in these runs was firstly

* A list of pyroxene analyses is obtainable by writing to the authors.

TABLE 1

Details of experiments and chemical ranges of pyroxenes (number of analyses are shown in parentheses)

Run. No.	P (kbars)	T (°C)	Time (hours)	Starting composition	H_2O	Products	Chemical range ($CaMgSi_2O_6$ mole %)	
							orthopyroxene	clinopyroxene
1	40	1200	4	$En_{50}Di_{50}$	*	EnDi	2.6– 5.6 (14)	88.0– 89.4 (10)
2	30	1200	0.1	$En_{50}Di_{50}$	anhydrous	EnDi		
3	30	1200	0.75	$En_{50}Di_{50}$	anhydrous	EnDi	6.0–11.6 (4)	71.2– 77.0 (5)
4	30	1200	4	$En_{50}Di_{50}$	*	EnDi glass	4.8– 6.4 (10)	85.8– 88.4 (13)
5	30	1200[2]	170	synthetic EnDi	*	EnDi glass	2.2– 6.2 (15)	84.2–100.0 (15)
6	10	1200	4	$En_{50}Di_{50}$	*	EnDi glass (tr)	7.4–10.0 (10)	78.6– 82.4 (10)
7	5	1200	4	$En_{50}Di_{50}$	*	EnDi glass Ol?	9.4–12.2 (10)	71.4– 77.6 (10)
8	5	1200	11	$En_{50}Di_{50}$	*	EnDi glass(tr)	9.6–12.6 (10)	74.8– 80.0 (10)
9	30	1500	2.5	$En_{50}Di_{50}$	*	clinopyroxene		45.6– 55.0 (12)
10	30	1200/1500	2.5/2.0	$En_{50}Di_{50}$	*	EnDi glass (tr)	6.4–10.2 (11)	55.4– 67.6 (16)
11	30	1500[2]	3.2	$En_{80}Di_{20}$	anhydrous	EnDi Qz?	10.4–11.6 (10)	49.6– 57.6 (10)
12	30	1200/1500[2]	2.1/4.2	$En_{80}Di_{20}$	anhydrous	EnDi	9.0–10.0 (6)	57.8– 68.2 (8)
13	30	900	23	$En_{50}Di_{50}$	a few %	EnDi Amph	1.6– 2.6 (12)	91.0– 92.8 (7)
14	30	900	214	synthetic EnDi	3%[1]	EnDi Amph (tr) magnesite (tr) Qz(tr)	0.2– 1.6 (5)	93.4– 99.8 (25)
15	10	900	72	$En_{50}Di_{50}$	a few %	EnDi	4.2– 6.4 (6)	76.4– 87.8 (15)
16	10	900	212	synthetic EnDi	4%[1]	EnDi Qz(tr)	1.4– 2.8 (9)	93.2– 98.8 (11)

* Starting materials were slightly moistened by breathing.

[1] 22% silver oxalate was also added.

[2] In the middle of the experiment indicated temperature decreased possibly due to chemical contamination of the thermocouple, and temperature was then controlled by maintaining power equal to the earlier condition. In run 5, an accidental "correction" of +70°C occurred for less than 1 hour after 100 hours of the experiment.

to single-phase clinopyroxene with composition similar to that of the starting glass, then nucleation of orthopyroxene and change of clinopyroxene towards the equilibrium composition, as in runs 2–4 and 7, 8 in Table 1. It is apparent that a glass with a composition within the pyroxene solvus crystallizes rapidly to form clinopyroxene of compositions similar to the glass composition, then or at the same time orthopyroxene nucleates, and the composition gap between the two pyroxenes widens until the solvus limit is reached.

In contrast to glasses, starting material of synthetic diopside ($CaMgSi_2O_6$) and enstatite or clinoenstatite ($Mg_2Si_2O_6$) react inwards until the solvus limits are reached. This is well demonstrated by the experiments in which layers of diopside and clinoenstatite were allowed to react across their boundary surface. In runs 5, 14 and 16, the $CaMgSi_2O_6$ content of diopside

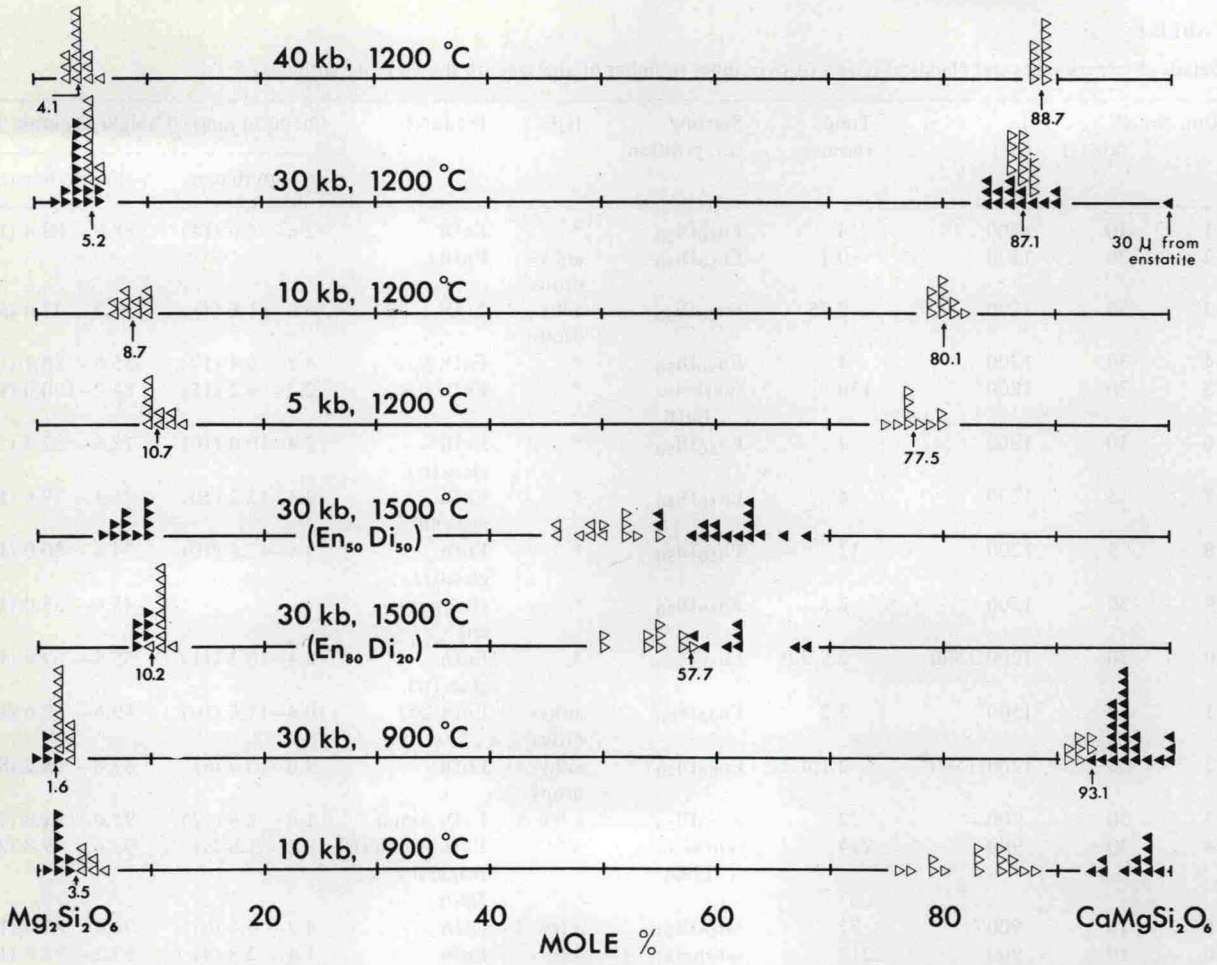

Fig. 1. Microprobe analyses of pyroxenes. Filled and open symbols are of homogenization and unmixing experiments, respectively. Decimal fractions in the raw data have been rounded to the nearest integer. Selected compositions are shown with arrows (see text).

30 μm from the boundary was 100%, and rapidly decreased to the boundary zone (10 μm) in which orthopyroxene occurred. The $CaMgSi_2O_6$ content of enstatite decreased away from the boundary zone and approached $Mg_2Si_2O_6$ at the other end. Additional examples of the inward reaction of natural pyroxenes towards the solvus are found in Hensen [11].

Thus, a pair of unmixing and homogenization experiments establishes or limits the position of a solvus even if chemical hysteresis remains and the data in either of the experiments are themselves scattered between starting composition and equilibrium composition.

Both unmixing and homogenization experiments were done at 30 kbars and 1200°C, 30 kbars and 900°C, 10 kbars and 900°C, and 30 kbars and 1500°C (Fig. 1), the last of which is separately discussed in the next section. The pair of experiments at 30 kbars and 1200°C yielded an overlap of the data by two experiments (Fig. 1). At 30 and 10 kbars at 900°C, the data could limit positions of solvus within analytical error except for the clinopyroxene limb at 10 kbars and 900°C where either the unmixing or homogenization experiments (or both) did not reach solvus and its position was only bracketted between $En_{12.2}Di_{87.8}$ and $En_{6.8}Di_{93.2}$.

At 40, 10 and 5 kbars at 1200°C, only unmixing experiments were made. Inferred solvus positions at these conditions are averages of the data.

5. Stability of subcalcic clinopyroxene at 30 kbars and 1500°C

There are four runs which are relevant to the problem of stability of subcalcic clinopyroxene found by Davis and Boyd [4]: runs 9 and 10 are on $En_{50}Di_{50}$, and runs 11 and 12 are on $En_{80}Di_{20}$. In runs 10 and 12, the charges were first kept at 1200°C and 30 kbars for a time considered sufficient (runs 2–4) to bring all the pyroxene compositions outside the solvus of 1500°C and 30 kbars, then temperature was increased to 1500°C. Thus, runs 9 and 10, and runs 11 and 12 can be regarded as pairs of unmixing and homogenization experiments. The results of runs 11 and 12 define the solvus very well. Run 9, however, resulted in a single-phase clinopyroxene and is inconsistent with run 10 where two pyroxenes remained and did not homogenize to a single phase. Two analyses of clinopyroxene in run 10 are slightly inconsistent with the solvus defined by runs 11 and 12, but only 15°C difference between them would explain the inconsistency. This choice of the solvus is in agreement with the data of Nehru and Wyllie [7] who carried out synthesis experiments using sintered gel of $En_{50}Di_{50}$ as starting material (Fig. 2).

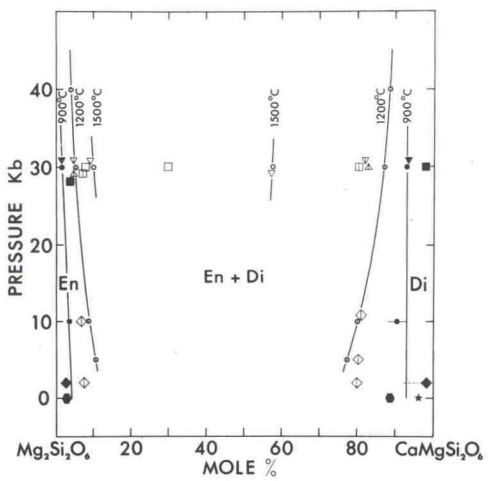

Fig. 2. Pressure-composition diagram of the enstatite–diopside solvus. Data are from Fig. 1 (circle, microprobe), Davis and Boyd [4] (square, optical), Boyd [5] (triangle, microprobe), Boyd and Schairer [1] (star, optical and X-ray), Atlas [14] (hexagon, X-ray), Warner and Luth [6] (diamond, X-ray), and Nehru and Wyllie [7] (inverted triangle, microprobe). Open symbols are at 1500°C, those with vertical line are at 1200°C, and the solid symbols are at 900°C. Some data at 10 and 30 kbars are plotted above or below the actual pressure to avoid confusion. En = enstatite, Di = diopside.

Generally, in unmixing runs yielding two pyroxenes, measured chemical ranges may be attributed to incomplete unmixing reactions, but if the single-phase pyroxene in run 9 were stable, there would be no reason for it to show such a wide chemical range as shown in Fig. 1. In run 11, two pyroxenes appeared within 3.2 hours, a slightly longer run duration than run 9, but the difference in run time appears unlikely to explain the absence of orthopyroxene. It is highly probable that $En_{50}Di_{50}$ is within the metastable composition range where Ca–Mg internal diffusion fails to occur at this P–T condition [12].

Further support for the revised position of solvus at 1500°C and 30 kbars is found in a partial melting experiment on natural garnet lherzolite [13]. In this run, clinopyroxene coexists with orthopyroxene as well as olivine, spinel and glass. The composition of the clinopyroxene ($Ca_{29.3}Mg_{66.2}Fe_{4.5}$, Al_2O_3 = 5.3%) is near to the revised solvus. Since Al_2O_3 solid solution stabilizes a wider solvus [5], correction for the Al_2O_3 effect in their result will move the composition of the clinopyroxene even closer to the solvus defined above. Thus the experiment in the multicomponent system supports the stability and wide solvus between two pyroxenes at 30 kbars and 1500°C in the simple system.

6. Temperature and pressure effects on the enstatite–diopside solvus

The positions of the solvus determined in preceding sections and shown in Fig. 1 are plotted on the pressure–composition diagram (Fig. 2) and temperature–composition diagram (Fig. 3). Available data from the literature are also shown. These data were obtained by three methods: optical identification of minerals in experimental charges, X-ray calibration of pyroxene composition, and microprobe analysis of pyroxenes. It should be noted that all the data plotted in both the figures are the respective authors' ultimate selections after statistical treatment or simple curve fittings, and are not their raw data which often deviate from the selections.

Accuracy of the first method depends on the quality of identification of minerals and the spacing of the

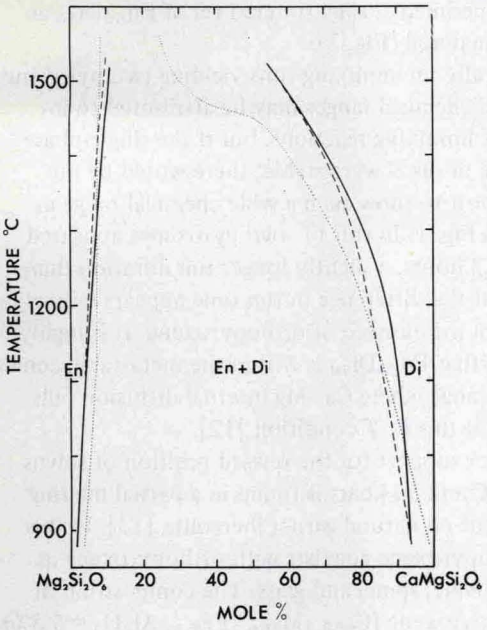

Fig. 3. The enstatite–diopside solvus at 30 kbars. Solid line: our data, dotted line: Davis and Boyd [4], and dashed line: Nehru and Wyllie [7].

composition grid employed, and that of X-ray method is ±1 to ±3 mole % end member [6,14]. The inconsistency seen among the data including ours should be viewed in relation to the accuracy of the method employed and the type of reaction, i.e. homogenization or unmixing. Particularly, it should be noted that determination of pyroxene composition from homogenization experiments using the X-ray calibration is very uncertain. This is because, in those experiments, chemical hysteresis can hardly be avoided, and the X-ray method will bias towards compositions outside the solvus.

The differences between the various data plotted in Fig. 2 are not entirely within analytical or method-derived error. We will examine particularly the data for the clinopyroxene limb at 1200°C and 30 kbars and at 900°C, 30 kbars to 1 atmosphere. Our reversal experiments at 30 kbars and 1200°C yielded overlapping compositional ranges with the unmixing experiment (run 4) giving strongly clustered data. We consider that the spread of the homogenization (run 5) data to lower diopside contents is due to greater temperature uncertainty in this run (see Table 1). In Fig. 2 we have drawn the solvus at 1200°C as a function of pressure as defined by our own data.

At 900°C and 30 kbars our closely bracketted reversal gives a clinopyroxene composition coincident with that predicted by extrapolation of Nehru and Wyllie's [7] data (1500–1000°C) and this composition is less calcic than that previously accepted [4]. At 900°C and 10 kbars our data bracket the clinopyroxene limb of the solvus within 5 mole % end member. At 900°C and 2 kbars earlier data [6] led to selection of a more calcic composition but it should be noted that in their unmixing experiments, Warner and Luth [6] did not obtain clinopyroxene more calcic than En_8Di_{92} (Fig. 2). The clinopyroxene limb at 900°C has been drawn through the reversal brackets at 30, 10 and 2 kbars but its extrapolation is then inconsistent with 1-atmosphere data [1,14]. Boyd and Schairer's [1] determination was based on optical identification of phases and some of the crucial phase identifications at and below 900°C were reported as doubtful (queried) [1, table 5]. Their data thus permit the interpretation that the clinopyroxene limb at one atmosphere lies between $En_{5.3}Di_{94.7}$ and $En_{10.7}Di_{89.3}$. We conclude, in the light of this and earlier studies, that there is little or no pressure effect on the diopside limb of the pyroxene solvus at 900°C from 0 to 30 kbars.

To summarize (Fig. 2), at higher temperature ($\geqslant$1200°C) the pyroxene solvus widens considerably as pressure increases, and at low temperature ($\leqslant$900°C) there is no perceptible pressure effect on the clinopyroxene limb and a slight pressure effect on the orthopyroxene limb. The pressure dependence of the orthopyroxene limb is of the same character as inferred in the Fe-bearing system [11]. Although pressure effects on emf of the thermocouple have not been corrected for and remain uncertain, the correction would raise indicated temperature to higher real values and would thus enhance the widening of the solvus with increasing pressure.

The temperature dependence of the solvus is shown in Figs. 2 and 3 which reaffirm the well-established increase of mutual solubility with increasing temperature. At 30 kbars, however, the shape of the re-determined solvus is very different from that of Davis and Boyd [4] and similar to that of Nehru and Wyllie [7]. Our new data show that the clinopyroxene limb is less sensitively dependent on temperature between 900 and 1200°C. This means that the

pyroxene geothermometer is less effective between 900 and 1200°C at high pressure than previously accepted.

7. Some problems in petrologic applications to natural pyroxenes

Applying Figs. 2 and 3, one may in theory estimate both pressure and temperature simultaneously from chemistry of coexisting enstatite and diopside. However, this is impractical as the isochemical contour lines for the two pyroxenes are nearly parallel throughout the P–T field except at temperatures above 1200°C where the two lines cross with a rather high angle between them. Even at high temperature, however, the application of this method to natural pyroxenes requires a full understanding of chemical effects in the multicomponent system. Consequently, the enstatite–diopside solvus can be used as a geothermometer only if the pressure of formation is estimated by another method, except in those cases where temperature is so low that the clinopyroxene limb is independent of pressure.

Application of the present results will necessitate revision of many temperature estimates found in the literature, particularly for assemblages of low-temperature peridotites and granulites and for high-pressure, high-temperature assemblages such as peridotite nodules in kimberlites. For example, estimates of temperature in the range 1200–1400°C at 30 kbars based on Davis and Boyd [4] would be revised upwards by about 100°C based on Fig. 3. An estimate of 1000°C at 30 kbars would be little changed but estimates of 900°C at 30 kbars would be revised downwards by more than 100°C. We emphasize, however, that data on the multi-component pyroxene system are required before unambiguous P–T determinations can be obtained for natural two-pyroxene assemblages.

8. Phase relations of pyroxenes in the system $Mg_2Si_2O_6$–$CaMgSi_2O_6$

Not only are enstatite and diopside stable in the system $Mg_2Si_2O_6$–$CaMgSi_2O_6$, but at least two more

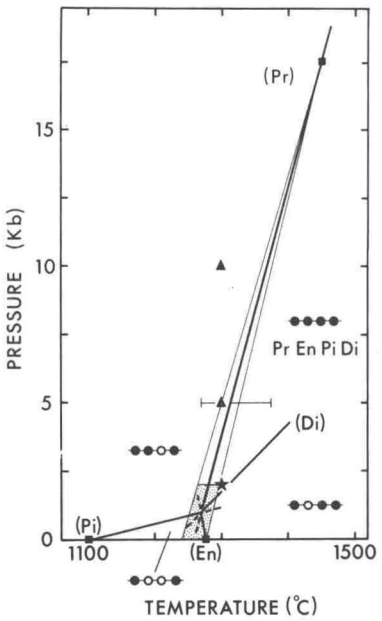

Fig. 4. An arrangement of the univariant lines around the invariant point where protoenstatite, enstatite, pigeonite and diopside coexist. Each line is identified by the missing phase from the invariant assemblage. Composition-assemblage diagrams are shown in each divariant field with, from left to right: Pr = protoenstatite, En = enstatite, Pi = pigeonite, Di = diopside. Open circle: unstable phase, filled circle: stable phase.

Data: squares [1,18,20], a bracket at 5 kbars [18], triangles: enstatite and diopside assemblage is stable [6], star: either enstatite–diopside, or pigeonite-bearing assemblage is stable [6,18]. See text for discussions.

stable phases exist, protoenstatite and pigeonite*. Protoenstatite is restricted to a low-pressure, high-temperature region [2,16]. Recent work by Smyth [17] reported protoenstatite of the composition $Mg_2Si_2O_6$ is stable up to melting point at 1 atm. Pigeonite appears over a wide P–T range from 1 atm to at least 20 kbars [2,18,19].

Three univariant assemblages known to occur are protoenstatite–enstatite–diopside at 1 atm and about 1100°C [1], enstatite–pigeonite–diopside at 17.5 kbars and 1450°C [18], and protoenstatite–pigeonite–diopside at 1 atm and about 1230°C [2]. For conditions for the last assemblage, the temperature, 1276°C [20], was preferred. This choice, in spite of

* This mineral is called iron-free pigeonite in the literature but the term "pigeonite" is used in this paper for convenience.

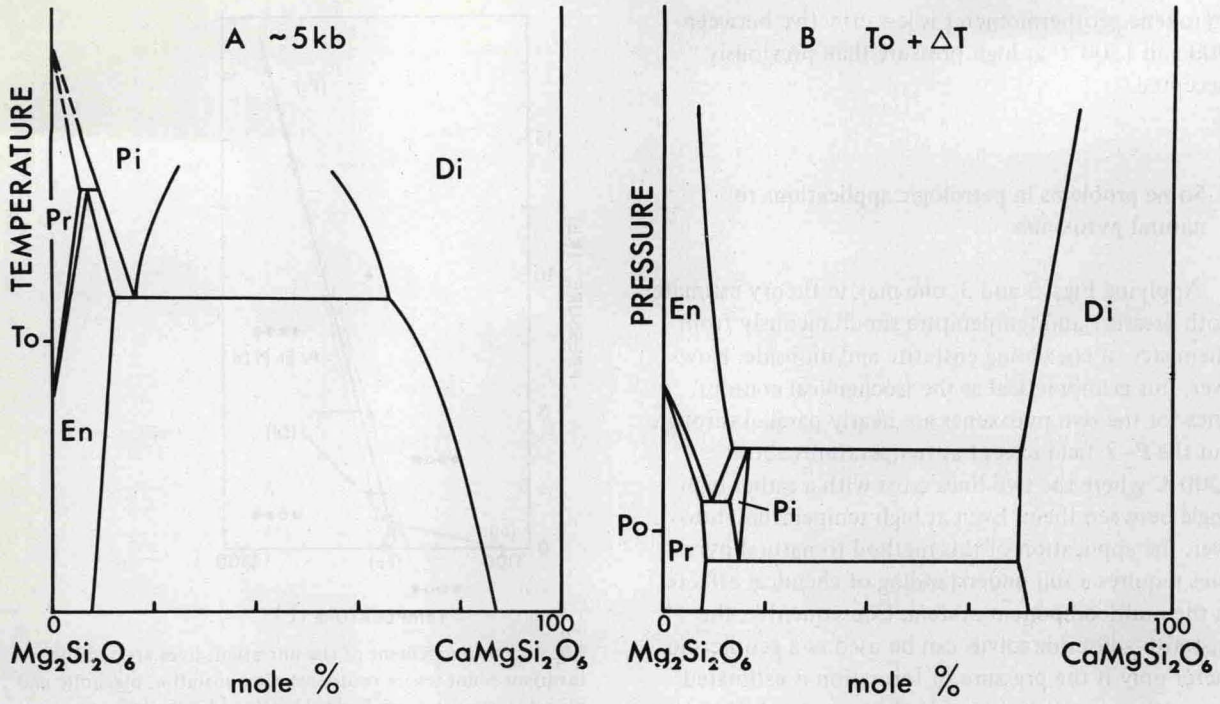

Fig. 5. A. A schematic phase diagram at about 5 kbars. B. A schematic phase diagram at just above T_0, based on the assumption that the slope of the univariant line (En) is negative as shown in Fig. 4.

the presence of Al_2O_3 in the system studied by Yang [20] was made because the coexistence of protoenstatite, pigeonite and diopside was confirmed at that temperature, and the Al_2O_3 content of less than 0.5 wt.% in the pyroxenes should have little effect on the temperature of the equilibrium. An invariant assemblage of all the four pyroxenes almost certainly occurs and Warner and Luth [6] estimate this to be at about 2 kbars and 1320°C.

A geometrical arrangement of four univariant lines around the invariant point is obtained following Schreinemakers' method [21]. An assumption here is that the $CaMgSi_2O_6$ content of pyroxenes at the invariant point increases in the order protoenstatite, enstatite, pigeonite, diopside. The shaded area in Fig. 4 limits the conditions for the invariant point. This area is partly defined by: (1) demands by the arrangement of the univariant lines, (2) three fixed points noted above, (3) a bracket for the univariant line (Pr) at 5 kbars [18], and (4) stability of enstatite and diopside at 10 and 5 kbars and 1300°C [6].

The nature of the stable assemblage at 2 kbars and 1300°C is confusing: it is enstatite and diopside (homogenization experiment) or pigeonite-bearing assemblage (unmixing experiment) [6,18]. This confusion might imply that a reaction, pigeonite = enstatite + diopside, characteristic of the univariant line (Pr), occurs near 2 kbars and 1300°C. If so, the invariant point will be further restricted to less than 2 kbars.

The deviation of the area thus restricted from Warner and Luth's estimate [6] is small but critical: their value implies that (En) is at a higher temperature than 1320°C at 1 atm [6, Fig. 5]. In fact it is not [2,20]. The conditions of the invariant point are hereafter referred to as P_0 and T_0.

It is now easy to draw the geometry of phase diagram at any T–P conditions. Fig. 5A, B shows examples at constant pressure and temperature around P_0 and T_0. They are only schematic, and partly exaggerated. Fig. 5B is drawn on an assumption that the slope of (En) is negative. A positive slope removes the protoenstatite–diopside solvus from the figure. The detail of the phase relations around P_0, T_0 must be determined by experiments, which should be concentrated in the shaded area (Fig. 4). However, such experiments will be extremely difficult because of

the difficulties in fine P–T control, sluggish reaction rate and appearance of metastable phases.

The univariant line (Pr) will be extrapolated to about 1590°C at 30 kbars (Fig. 4), which means that pigeonite becomes stable at this condition. Thus, as Kushiro [3] suggested, some of the subcalcic clinopyroxenes coexisting with orthopyroxene at high temperatures in the phase diagram by Davis and Boyd [4] are possibly pigeonite and the diopside–pigeonite solvus should appear at temperatures higher than about 1590°C. This interpretation is similar to that for pyroxenes in the system $Fe_2Si_2O_6$–$CaFeSi_2O_6$ at 20 kbars [22].

Acknowledgements

The authors are grateful to G.M. Biggar, University of Edinburgh, for constructive discussions, to F.R. Boyd (Geophysical Lab.), A.E. Ringwood, and G. Brey (A.N.U.) and M. Obata (M.I.T.) for critical reading of a manuscript at an early stage, and to W.O. Hibberson, N.G. Ware and E.H. Pedersen for technical assistance with experiments.

Appendix. Run details

Run 1 (40 kbars, 1200°C, unmixing from glass). Enstatite and diopside were commonly euhedral, up to 70 μm in grain size and in some cases in parallel growth or as inclusions one within the other.

Run 2 (30 kbars, 1200°C, unmixing). Within 6 minutes, all the starting glass crystallized into pyroxenes. They were identified optically and by X-ray as minor enstatite and common diopside, but were too small for microprobe analysis.

Run 3 (30 kbars, 1200°C, unmixing). Enstatite and diopside grew up to 20 μm.

Run 4 (30 kbars, 1200°C, unmixing). Enstatite (up to 50 μm) and diopside (up to 20 μm) were subhedral to euhedral. About 20% of glass was present.

Run 5 (30 kbars, 1200°C, homogenization). At the interface between diopside and enstatite layers in the capsule, pyroxenes with two different textures were found, i.e. orthoenstatite and diopside crystals as large as the original synthetic pyroxenes (30 μm), and small pyroxenes (≤8 μm) interpreted as products of new nucleation of pyroxene. Both types of pyroxene were analyzed.

No clinoenstatite remained after the experiment. However, at one corner of the capsule originally occupied by diopside, partial melting occurred and euhedral enstatite (80 μm) were formed. The glass contained 11% Al_2O_3, 0.3% Na_2O and 0.5% K_2O. This contamination may be due to fracturing of the capsule during the run, with exposure to the ceramic enclosing the capsule. Contamination by Al_2O_3, Na_2O or K_2O, however, was not detected in the diopside even where directly contacting the glass.

Run 6 (10 kbars, 1200°C, unmixing). Enstatite and diopside were ≤30 μm in grain size and there was a small amount of glass.

Run 7 (5 kbars, 1200°C, 4 hours, unmixing). Enstatite, diopside, glass, and probably minor olivine occurred in anhedral texture.

Run 8 (5 kbars, 1200°C, 11 hours, unmixing). Enstatite (≤30 μm) and diopside (≤15 μm) occurred as subhedral crystals, probably with trace amounts of glass. Some diopside crystals are simply twinned. The diopside is more calcic than that in run 5 (Table 1) and this run is preferred to run 7.

Run 9 (30 kbars, 1500°C, unmixing). Only clinopyroxene was observed optically, as subhedral grains up to 30 μm in grain size.

Run 10 (30 kbars, 1500°C, homogenization). A glass ($En_{50}Di_{50}$) was subjected to 30 kbars and 1200°C for 2.5 hours and then the temperature was raised to 1500°C for 2 hours. From runs 2–4 we infer that the charge crystallized to two pyroxenes with a wide composition gap at 1200°C and that these pyroxenes then approached re-equilibration at 1500°C. Euhedral diopside and enstatite (up to 20 μm) and a trace amount of glass were produced

Run 11 (30 kbars, 1500°C, unmixing). A glass of $En_{80}Di_{20}$ yielded euhedral enstatite (up to 50 μm) with small anhedral or subhedral diopside.

Run 12 (30 kbars, 1500°C, homogenization). The same techniques as for run 10 were used for a glass of $En_{80}Di_{20}$ composition. Some enstatite crystals were up to 30 μm long and had parallel growth of diopside. Diopside was generally much smaller and anhedral.

Run 13 (30 kbars, 900°C, unmixing). Enstatite was frequently acicular (up to 70 μm long) while diopside was equant and ≤15 μm. An amphibole ($Ca_{3.2}Mg_{3.8}Si_{8.0}O_{23}$) occurred and is probably metastable (judged by its unusual composition).

Run 14 (30 kbars, 900°C, homogenization). Originally, in order to try both homogenization and unmixing experiments at one time, layers of synthetic diopside, clinoenstatite and glass ($En_{50}Di_{50}$) were loaded successively into the capsule. However, the unmixing experiment in the glass layer proved am-

biguous and unusable because of mechanical contamination of the synthetic pyroxenes into this layer during loading, and eventually only the homogenization experiment was usable. To minimise the likelihood of amphibole stability in the presence of approximately 3% H_2O, about 22% silver oxalate was mixed into each layer. However, amphibole of similar composition to that in run 13 was formed locally at the boundary between synthetic pyroxene layers, and within the glass layer. Trace amounts of silica mineral and magnesite were formed as well. Very small pyroxenes appeared to have nucleated at the enstatite/diopside boundary but were difficult to distinguish from relict grains.

Run 15 (10 kbars, 900°C, unmixing). Enstatite ($\leqslant 10\mu m$) and diopside ($\leqslant 5\ \mu m$) were so fine grained that it is not clear whether the wide compositional range of diopside (Table 1) is real, and due to incomplete equilibration, or results from enstatite contamination in the diopside analyses.

Run 16 (10 kbars, 900°C homogenization). The same preparation of the starting material, together with water and silver oxalate, was used as in run 14 and the unmixing experiment was unsuccessful for the same reason. At the boundary between the two synthetic pyroxene layers, the same texture was present as in run 14. Two pyroxenes and a trace of silica mineral were present.

References

1 F.R. Boyd and J.F. Schairer, The system $MgSiO_3$–$CaMgSi_2O_6$, J. Petrol. 5 (1964) 275.

2 I. Kushiro, Determination of liquidus relations in synthetic silicate systems with electron probe analysis: the system forsterite–diopside–silica at 1 atmosphere, Am. Mineral. 57 (1972) 1260.

3 I. Kushiro, The system forsterite–diopside–silica with and without water at high pressures, Am. J. Sci. Schairer Vol. 267-A (1969) 269.

4 B.T.C. Davis and F.R. Boyd, The join $Mg_2Si_2O_6$–$CaMgSi_2O_6$ at 30 kilobars pressure and its application to pyroxenes from kimberlites, J. Geophys. Res. 71 (1966) 3567.

5 F.R. Boyd, Garnet peridotites and the system $CaSiO_3$–$MgSiO_3$–Al_2O_3, Mineral. Soc. Am. Spec. Pap. 3 (1970) 63.

6 R.D. Warner and W.C. Luth, The diopside–orthoenstatite two-phase region in the system $CaMgSi_2O_6$–$Mg_2Si_2O_6$, Am. Mineral. 59 (1974) 98.

7 C.E. Nehru and P.J. Wyllie, Electron microprobe measurement of pyroxenes coexisting with H_2O^- under saturated liquid in the join $CaMgSi_2O_6$–$Mg_2Si_2O_6$–H_2O at 30 kilobars, with applications to geothermometry, Contrib. Mineral. Petrol. 48 (1974) 221.

8 S.J.B. Reed, and N.G. Ware, Quantitative electron microprobe analysis using a Lithium drifted silicon detector, X-ray Spectrom. 2 (1973) 69.

9 F.R. Boyd and J.L. England, Apparatus for phase equilibrium measurements at pressures up to 50 kb and temperature up to 1750°C, J. Geophys. Res. 65 (1960) 741.

10 T.H. Green, A.E. Ringwood and A. Major, Friction effects and pressure calibration in a piston cylinder apparatus at high pressure and temperature, J. Geophys. Res. 71 (1966) 3589.

11 B.J. Hensen, Pyroxenes and garnets as geothermometers and barometers, Carnegie Inst. Wash. Year Book 72 (1973) 527.

12 J.B. Thompson Jr., Thermodynamic properties of simple solutions, in: Researches in Geochemistry, 2, P.H. Abelson, ed. (New York, 1967) 340.

13 I. Kushiro, N. Shimizu, Y. Nakamura and S. Akimoto, Compositions of coexisting liquid and solid phases formed upon melting of natural garnet and spinel lherzolites at high pressures: a preliminary report, Earth Plan. Sci. Lett. 14 (1972) 19.

14 L. Atlas, The polymorphism of $MgSiO_3$ and solid-state equilibria in the system $MgSiO_3$–$CaMgSi_2O_6$, J. Geol. 60 (1952) 125.

15 I.C. Getting and G.C. Kennedy, Effect of pressure on the emf of chromel-alumel and platinum-platinum 10% rhodium thermocouples, J. Appl. Phys. 41 (1970) 4552.

16 P. Anastasiou and F. Seifert, Solid solubility of Al_2O_3 in enstatite at high temperatures and 1–5 kb water pressure, Contrib. Mineral. Petrol. 34 (1972) 272.

17 J.R. Smyth, Experimental study on the polymorphism of enstatite, Am. Mineral. 59 (1974) 345.

18 I. Kushiro and H.S. Yoder, Jr., Stability field of iron-free pigeonite in the system $MgSiO_3$–$CaMgSi_2O_6$, Carnegie Inst. Wash. Year Book 68 (1970) 226.

19 H.Y. Yang and W.R. Foster, Stability of iron-free pigeonite at atmospheric pressure, Am. Mineral. 57 (1972) 1232.

20 H.Y. Yang, Crystallization of iron-free pigeonite in the system anorthite–diopside–enstatite–silica at atmospheric pressure, Am. Mineral. 273 (1973) 488.

21 E-An. Zen, Construction of pressure-temperature diagrams for multicomponent systems after the method of Schreinemakers – a geometric approach, Bull. U.S. Geol. Surv. 1225 (1966).

22 D.H. Lindsley and J.L. Munoz, Subsolidus relations along the join hedenbergite–ferrosilite, Am. J. Sci. Schairer Vol. 267-A (1969) 295.